CHAPTER IV

INVESTIGATION OF STRUCTURAL CHANGES RELATED TO TEMPERATURE: AN UNDERSTANDING OF H-BOND BASED PROTON TRANSFER IN 4-VINYLIMIDAZOLE AND ACRYLIC ACID COPOLYMER MEMBRANE

4.1 Abstract

An attempt to understand how proton transfer proceeds in poly (acrylic acid-co-4(5)-vinylimidazole) has been carried out based on the temperature dependent characterization techniques, i.e., Fourier transform infrared spectroscopy (FTIR), wide angle X-ray diffraction (WAXD), Raman spectroscopy, including the atomic distance calculations. Systematical studies are achieved from a series of poly (acrylic acid-co-4(5)-vinylimidazole) with different acrylic acid content. When the copolymer is almost an ideal in equimolar ratio of an alternating structure, the hydrogen bond between carboxylic acid and imidazole is maintained and initiates the proton conductivity even at 120 °C. Whereas when the copolymer is carboxylic acid rich, the dehydration to form anhydride proceeds resulting in the decrease in proton conductivity at high temperature. The radial distribution function (RDF) calculated from the WAXD pattern shows that the inter-atomic distances reflect how the increase in temperature induces a favorable packing structure under the hydrogen bond network and the chain mobility to enhance the proton transfer at high temperature, especially in the case of the copolymer with an ideal alternating structure.

Keywords: Acrylic acid; 4-Vinylimidazole; Radial distribution function; Proton conductivity; Polymer electrolyte membrane

4.2 Introduction

Nafion® is a successful traditional polymer electrolyte membrane fuel cell (PEMFC) for applications at low operating temperatures (~80 °C). The proton

hopping mechanism of the polymer electrolyte membrane has been investigated for a number of years [1,2]. Tsuda *et al.* reported the initial proton transfer involved a water molecule and a subsequent hydronium ion by hydrogen bonding between the aqueous media and SO_3^- of the Nafion side chains to reorganize and energetically stabilize the side chains. The proton transfer is favorably assisted via the H_2O molecules between SO_3^- groups, involving the internal conversion between covalent and hydrogen bonds [3]. In recent years, the criteria for PEM components especially in automobiles has been recognized [4,5]. A potential polymer membrane should give a proton conductivity of 0.1 S/cm at 120 °C under preferably water-free conditions. The advantages of an operating temperature above 120 °C are, for example, improving CO tolerance at the anode [6], accelerating the reaction kinetics, and the ease of water management [7,8]. Heterocyclic molecules such as imidazole or pyrazole which are known as key molecules in enzymatic biological membranes are in expectation as molecules to function in the membranes for fuel cells. For example, imidazole has a high boiling point and is reported as a functional group for proton transfer [9,10]. A Nafion/imidazole recast membrane has been demonstrated to have a proton conductivity of ~0.1 S/cm at 160–180 °C. However, this imidazole-impregnated recast Nafion® could not improve current density since it poisoned the platinum electrocatalyst as studied in cyclic voltammetry [11]. Several attempts have been made to make new materials to overcome the incompatibility of imidazole with a platinum catalyst. One way is by incorporating imidazole into the hydrocarbon main chain such as 4(5)-vinylimidazole followed by blending with sulfuric or phosphoric acid [12,13]. Highly thermally stable polybenzimidazole doped with phosphoric acid showed a proton conductivity of ~ 5×10^{-2} S/cm [14]. Imidazole-terminated ethyleneoxide oligomers were created to be model materials giving a conductivity of up to 5×10^{-3} S/cm at 120 °C [15]. Based on the concept of proton donor and acceptor in polymer matrices, copolymer membranes of ethyleneglycol methacrylate phosphate and 4(5)-vinylimidazole were synthesized and the proton conductivity was found to be ~10^{-4} S/cm at 160 °C [16]. Bozkurt et al. proposed the preparation of copolymers of 4(5)-vinylimidazole and vinylphosphonic acid with a proton conductivity of ~10^{-6}–10^{-12} S/cm at 140 °C [17]. It is important to note that

although the approach to achieve new proton-conducting materials was developed, the understanding of the proton transfer at the molecular level related to the temperature is still a key point to improve membrane performance.

In previous, we reported the preparation of acrylic acid and 4(5)-vinylimidazole copolymer. The proton conductivity was as high as ~0.01 S/cm at 120 °C when 4(5)-vinylimidazole content was 66.6 %. However, the factors related to the changes in temperature and its consequent proton conductivity has not been yet investigated. The present work, thus, aims to clarify the possibility of proton transfer system under the variation of temperature. There, the copolymers with various acrylic acid and imidazole contents together with characterizations, especially FTIR, Raman spectroscopy, WAXD under the temperature controllable accessories were designed and carried out. The RDF calculated under the temperature changes also allows us to evaluate the morphological packing structure of the copolymer in the membrane matrices [18]. By considering the packing structure together with the proton conductivity data, it is for the first time we are able to overview the effectiveness of proton transfer mechanism related to the H-bond in the system.

4.3 Experimental Section

4.3.1 Chemicals

Urocanic acid and 2, 2'-azobisisobutyronitrile were purchased from Sigma Aldrich (USA). Methanol and acetone were obtained from Lab-Scan (Ireland). Acrylic acid and hydrochloric acid were purchased from Fluka Chemicals (Buchs, Switzerland). All chemicals were AR grade and used without further purification, except for the acrylic acid. Copolymer membranes of acrylic acid (AA) and 4(5)-vinylimidazole (4-VIm) were prepared with various copolymer ratios—1:4 (**M1**), 1:1 (**M2**), 4:1 (**M3**), and 19:1 (**M4**)—where x and y indicates the feed ratio of acrylic acid and 4(5)-vinylimidazole. In addition, the 4(5)-vinylimidazole content was found to be 66.6 %, 64.5 %, 28.6 %, and 4.2 % for **M1**, **M2**, **M3**, and **M4**, respectively [19].

4.3.2 Measurements

FTIR spectra were obtained by a Varian FTS 7000 series FTIR spectrometer at a resolution of 2 cm^{-1} in the region of 4000–400 cm^{-1}. The high temperature FTIR spectra were obtained by sandwiching the sample between KBr pellets. The spectra were collected at each desired temperature. The polarized Raman spectra were recorded in the region 4000–100 cm^{-1} with the resolution power of 2 cm^{-1} by a Japan Spectroscopic Co., NRS-2100, laser Raman spectrophotometer. The back-scattering geometry was used with a 532 nm laser beam.

WAXD patterns were measured by using a Rigaku X-ray diffractometer, D/MAX RINT-2000, with a Cu-Kα line as an incident X-ray beam. Membrane samples were adhered to a glass slide and measured at 2θ angles between 3° and 40° in steps of 0.02° with a scan speed of 0.1 °C/min. The dependence of temperature on the WAXD patterns was measured by using simultaneous WAXD and DSC Rigaku/MSC accessories at 2θ between 3° and 40° in steps of 0.02° with scan speed 1 °C/min. The 2-dimensional WAXD patterns were measured by a Rigaku Nanoviewer with Cu-Kα beam and an imaging plate.

Molecular dynamics (MD) calculation was performed on a single copolymer chain of acrylic acid and 4(5)-vinylimidazole having 20 monomer units with various copolymer contents according to **M1**, **M2**, **M3**, and **M4**. The thus-created polymer segments were linked at the end points to give an infinitely long chain under the periodic boundary condition. The size of the cubic cell was adjusted to have a density of 0.9 g/cm^3. The random coil was generated by using an amorphous builder of the commercial software Cerius^2 (Accelrys®). The MD calculation was performed under the constant NPT condition (N = number of atoms, P = pressure, and T = temperature). After minimizing the total energy using a force-field COMPASS, the MD calculation was performed at 298 K after equilibration of 30 ps for 100 ps.

Impedance measurements were performed using an Autolab/PGSTAT 30 analyzer in the frequency range from 10–10^5 Hz and 50 mV amplitude. The FRA2 module was controlled by FRA 4.9 software. The *through-plane* conductivity was measured by sandwiching membranes between gas diffusion electrodes (ELAT®

containing 0.25 mg Pt/cm^2) and copper disks. The conductivity of membranes was carried out as a function of temperature (from 25 to 120 °C) without any additional humidification. The impedance measurement was calibrated on the basis of the contribution of the empty and short-circuit cell. The membrane resistance was obtained from an extrapolation of the real axis on the high frequency part. The proton conductivity (σ) was recorded as the impedance value at zero phase angles.

4.4 Results and Discussion

4.4.1 Temperature dependence of copolymer structure

In our previous work, we succeeded in preparing acrylic acid and 4(5)-vinylimidazole copolymer. The characterization results informed an alternating copolymer structure which was relevant to the reactivity ratio (r) [19]. By varying the temperature, the proton conductivity was found to be increased in the case of **M1**. There, it is important to clarify how the structure, especially the morphology, changed and initiated the proton conductivity.

It should be noted that our copolymer possibly favors the hydrogen bond between carboxylic acid and 4(5)-vinylimidazole groups (see Scheme 4.1 (a)). This hydrogen bond might obstruct the copolymer to dissolve in general solvents except acids. In other words, we expect for the hydrogen bond functions in proton transfer mechanism.

Scheme 4.1 (a) Proton transfer of **M1** and **M4** by hydrogen-bonding network and (b) Non-cyclic anhydride formation of **M4** at temperatures above 150 °C

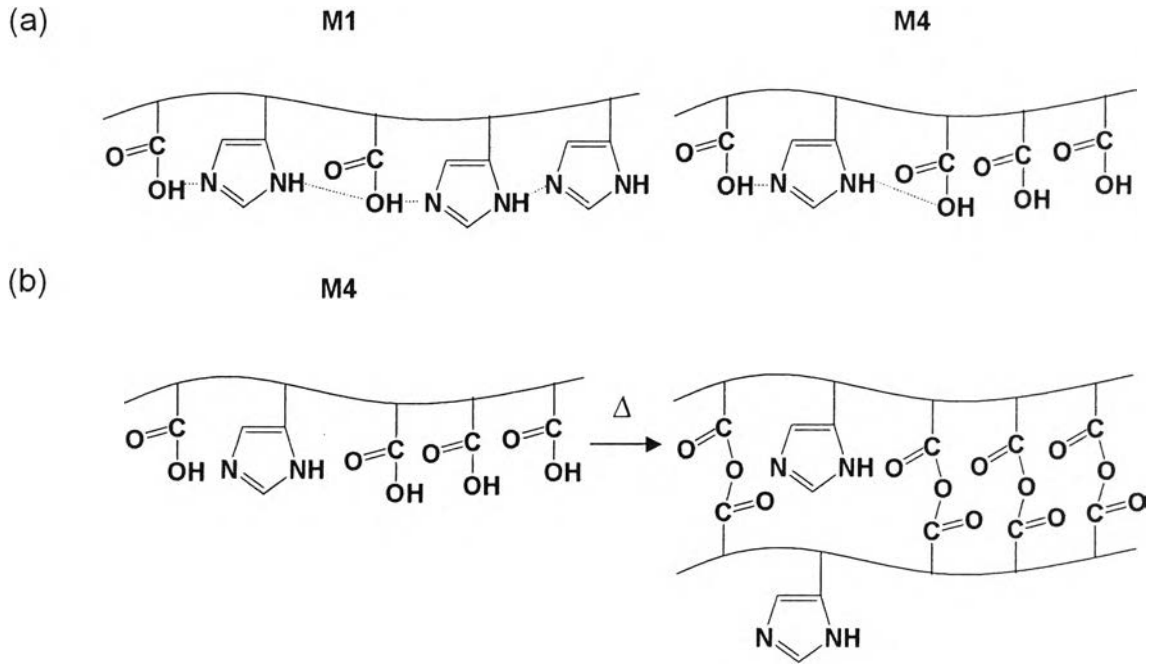

In order to investigate the structural changes, an in-house accessory for FTIR and Raman measurements were developed. The membrane was prepared by casting the copolymer in 1% hydrochloric acid solution. Figure 4.1 (a) shows the FTIR spectrum of each copolymer membrane at room temperature with significant peaks at ~2970–2880 cm^{-1} (CH_2 stretching), 3300-2500 cm^{-1} (NH--N), and ~3500–3300 cm^{-1} (OH--N or NH stretching) [20]. The hydrogen bonded NH--N band also appears in Raman spectra (see Figure 4.1 (b)) at 3143 cm^{-1} [21]. The peak intensity is interfered with OH group and shifts to 3160 cm^{-1} when the 4-VIm content was decreased, especially in the case of **M4**.

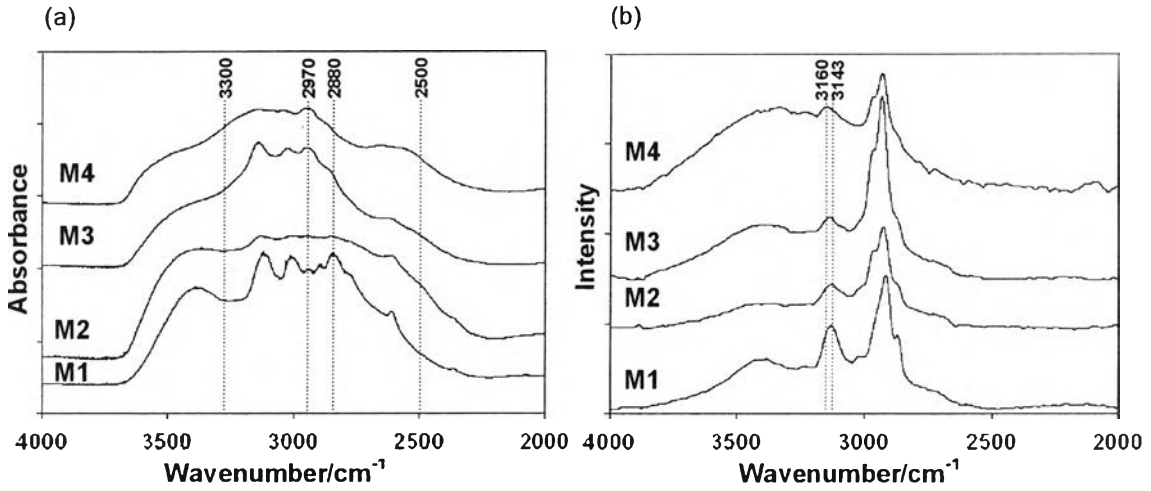

Figure 4.1 (a) FTIR and (b) Raman spectra of copolymer membranes, **M1**-**M4**, at room temperature.

Grothuss and vehicle mechanisms have been proposed for the hydrogen bonded based proton transfer mechanism [22–23]. In our case, as the FTIR spectra of the copolymers showed the hydrogen bond network, the studies on temperature dependency were carried out. The copolymer membranes were mounted in an in-house temperature controlled accessory and were heated from room temperature to 200 °C. Figure 4.2 (a) shows some FTIR spectra of **M1** and **M2** in the range of 4000–2000 cm^{-1} observed in every 10 °C increase starting from 20–200 °C. The formation of OH--NH bond band at 3450–3413 cm^{-1} is significantly decreased when the temperature increased and finally disappears at 150 °C. Figure 4.2 (b) shows a semi-quantitative plot of hydrogen bond peak in each membrane at the observed temperature (T_T) related to the room temperature (T_0). It is clear that **M1** and **M2** give a significant decrease of OH--NH peak from room temperature to 140 °C and to 120 °C whereas **M3** and **M4** show only a small decrease from room temperature to 60 °C and to 80 °C, respectively. This implies that (i) the thermal vibrational energy induces the loss in hydrogen bond between N-H and O-H, and (ii) the copolymers with an almost equivalent ratio of imidazole and acrylic acid content (**M1** and **M2**) form a good hydrogen bond network in the long range from room temperature to over 100 °C.

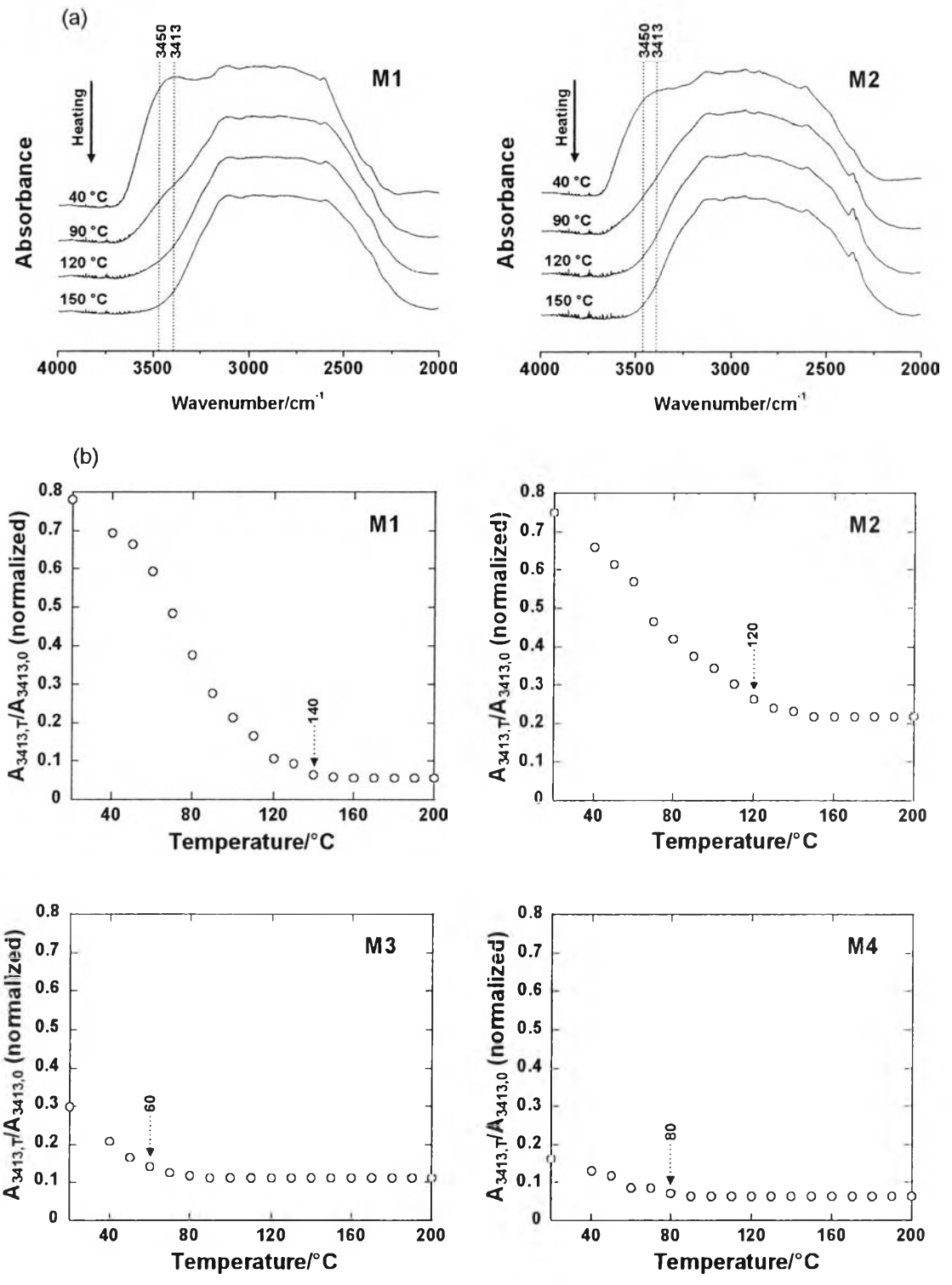

Figure 4.2 (a) FTIR spectra of **M1** and **M2** at various temperatures, and (b) Variation of the normalized absorbance at ν_{3413} of copolymers: **M1**, **M2**, **M3**, and **M4**.

In the cases of **M3** and **M4**, when the temperature increased, the FTIR bands at 1805 cm^{-1} (COO) (A_L) and 1060 cm^{-1} (COC) increase while the band at 920 cm^{-1} (C-OH) decreases (see Figure 4.3 (a)). The changes of COO and COC peaks imply an anhydride formation related to the temperature. Considering the C=O bands, the ratio of the peaks at 1805 cm^{-1} to 1740 cm^{-1} (A_H) refers to the unconjugated noncyclic anhydrides since the ratio is less than one [21]. This informs us that the thermal vibrational energy induces the carboxylic acid-rich copolymer membranes (**M3** and **M4**) to form a planar non-cyclic anhydride as a consequence of dehydration. Scheme 4 1 (b) shows a possible anhydride formation.

Figure 4.3 (b) is semi-quantitative plots of the peaks at 1805 cm^{-1} and 1060 cm^{-1} based on the room temperature (T_0) and the temperature in observation (T_T) to follow the anhydride formation when the temperature increases. It is clear that both peaks appear significantly after the membranes were heated above 150 °C. This reflects the dehydration of carboxylic acid to form anhydride group in polymer side chain.

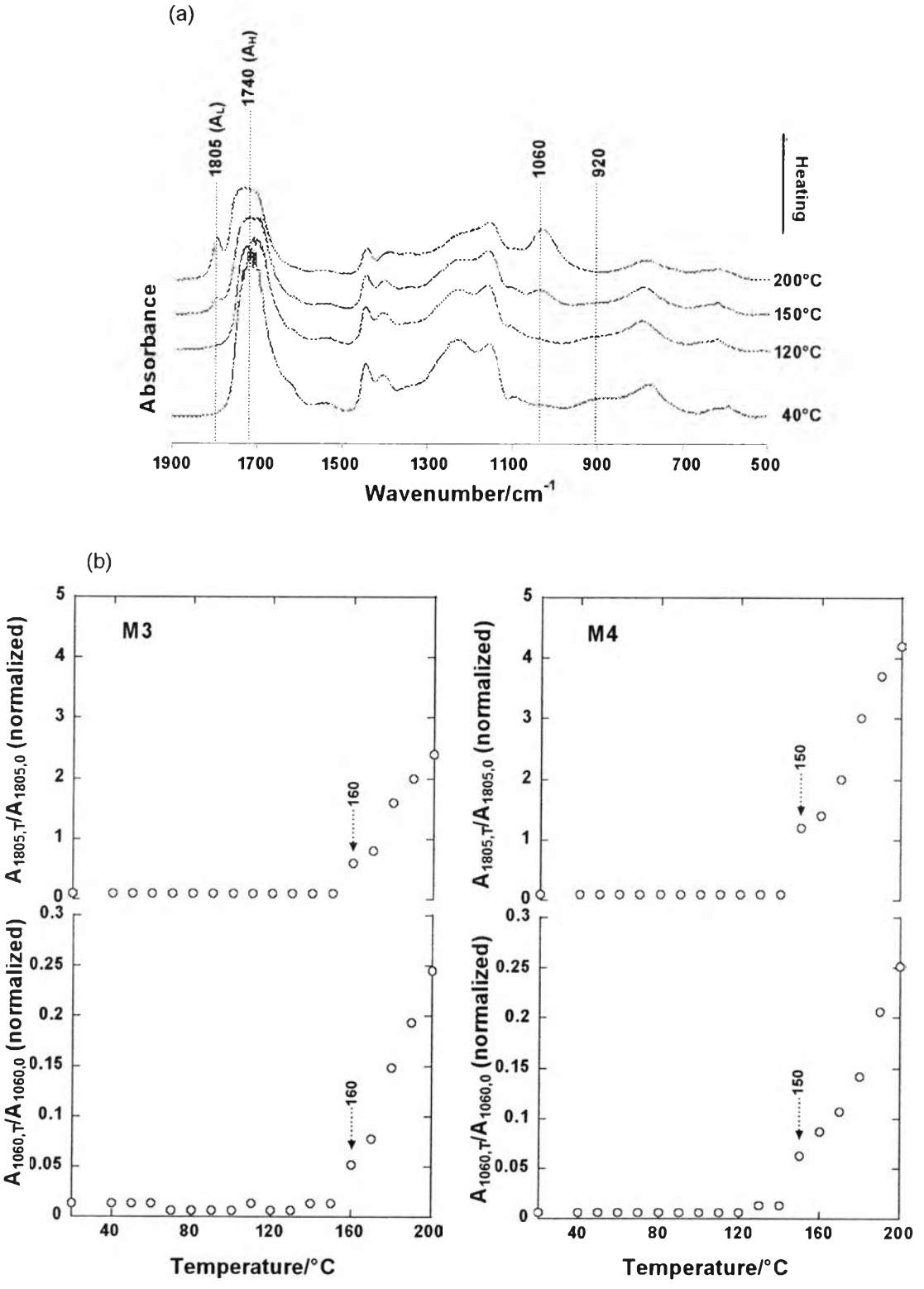

Figure 4.3 (a) FTIR spectra of **M4** at various temperatures (A_L = lower absorbance and A_H = higher absorbance), and (b) Variation of the normalized absorbance at ν_{1805} and ν_{1060} of copolymers: **M3** and **M4**.

4.4.2 Temperature dependence of WAXD

It is important to note that the preliminary measurement using 2D-WAXD technique showed that all the membranes gave the amorphous halos at room temperature. In order to investigate morphologies of the membranes related to temperature range, a series of WAXD patterns was observed using a temperature controlled accessory. For **M1–M2**, the broad peak from 17° to 23° 2θ was focused.

The peaks of all copolymer films in the range of 17–23° shifted to lower 2θ about 3–5° might be due to the thermal expansions. The changes of WAXD patterns were further used to quantitatively analyze by using RDF. The RDF gives the distribution of inter-atomic distances in term of magnitudes but not the direction of the inter-atomic vectors [24–25]. In addition, the RDF based on X-ray diffraction technique of the amorphous structure was used to obtain good quality interference functions. In our case, the peaks in differential RDF (DRDF) curves were suitably resolved, giving more precisely information than full width at half maximum (FWHM) [26]. The (DRDF) g(r) was calculated on the basis of the equation (1) using an scattering intensity i(q):

$$g(r) = 4\pi r^2[\rho(r)-\rho(o)] = (2r/\pi)\cdot\int q\cdot i(q)\cdot\sin(qr)\,dq \qquad (1)$$

where ρ_0 is the average atomic density in the sample and is directly deduced from the experimental density, $\rho(r)$ is the number of atoms per unit volume at a distance r from every other atom taken successively as the reference atom, and q is a scattering vector, $q = 4\pi\sin\theta/\lambda$.

The experimental intensities, I(q), were corrected for the background, polarization, and Lorentz factor by tabulating the incoherent scattering factor with weight fraction in order to obtain the scattering curve i(q), as described in equations (2)–(5):

$$I(q) = k\cdot I_{coh}(q)-\Sigma\, x_j f_j^2 \qquad (2)$$

$$i(q) = I(q)/\Sigma\, x_i f_i^2\,(q) \qquad (3)$$

$$i(q) = k\,[I_{coh}(q)/\Sigma\, x_j f_j^2(q)]-1 \quad (4)$$

$$k = 0.4142/(FWHM/2)^2 \quad (5)$$

where x_j is the mole fraction of species j, and $f_j(q)$ is the atomic scattering factor for atom type j. The hypothetical chemical units of ($C_{4.3}H_{5.3}O_{0.6}N_{1.3}$) for **M1**, ($C_{4.3}H_{5.3}O_{0.7}N_{1.3}$) for **M2**, ($C_{3.6}H_{4.6}O_{1.4}N_{0.6}$) for **M3**, and ($C_3H_4O_2N_{0.08}$) for **M4** were assumed based on the found compositions of the copolymers by ^{1}H-NMR [27–29]. I(q) is an observed intensity, and I_{coh} represents the coherently scattered intensity [30–31]. The k is a normalization constant needed to place the intensity on an absolute scale. The terminal effect of Fourier transform in equation (1) was erased relatively well by using a window function, M(q), given below [31]. Therefore, the DRDF can be calculated using equation (7):

$$M(q) = \sin(\pi q/q_{max})/(\pi q/q_{max}) \;; \quad q \le q_{max} \quad (6)$$
$$= 0 \qquad\qquad q > q_{max}$$

$$g(r) = 4\pi r^2[\rho(r)-\rho(o)] = (2r/\pi)\cdot\int q\cdot i(q)\cdot M(q)\cdot\sin(qr)\,dq \quad (7)$$

Generally, an RDF indicates the atomic or electronic density as a function of distance from every atom or electron in the system, estimating successively from the origin. The RDF with various inter-atomic distances consists of three main regions. The maxima in the range of $r < 3$ Å (zone A) refers to the intra-molecular regularities in the polymer chain. The maxima in the range $3 < r < 6$ Å (zone B) are interpreted as the intra- and inter-molecular pairs of atoms, and those for $r > 6$ Å (zone C) are attributed to the inter-molecular distances [32].

Figure 4.4 shows the temperature dependencies of the RDF calculated for the **M1**–**M4** copolymers. To simplify the curve, Figure 4.4 shows only 6 temperatures of the RDF fluctuation for all copolymers. It is not necessary to postulate the atomic distances beyond 14 Å due to the consistence of RDF plot. Based on equation (7), the first peak at 1.2 Å corresponds to the nearest neighbor distance between the chemically bonded atoms. This peak position for the first neighbor remains nearly the same in all temperature and all membranes (**M1**–**M4**), thus structural re-ordering

during heating to explain an increase in proton conductivity can be eliminated. In the case of **M4**, we found that the atomic density at 1.2 Å is significantly increased above 87 °C.

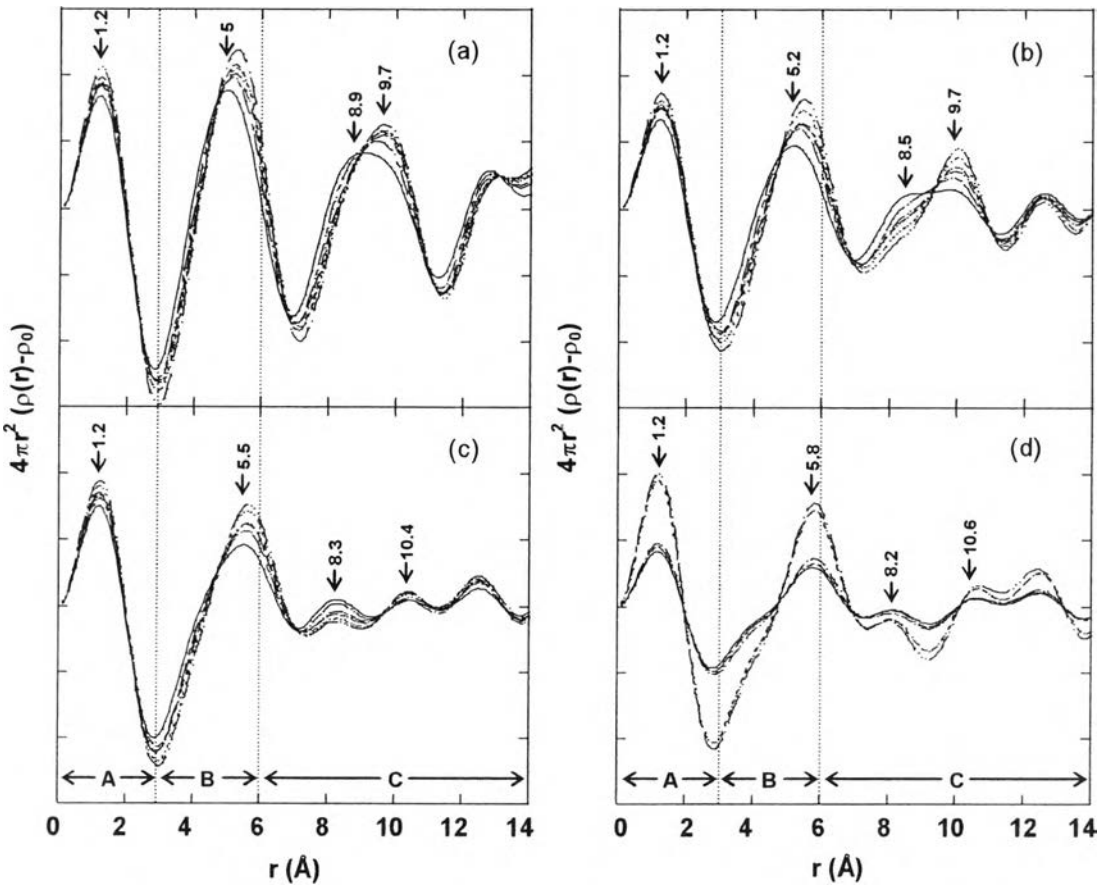

Figure 4.4 Differential radial distribution function (DRDF), $4\pi r^2 (\rho(r)-\rho_0)$, of the type of copolymers at various temperatures, _____ 38 °C, _..._.. 63 °C, _ _ _ _ 87 °C, _ _ _ _ _ 99 °C, ... 123 °C , _._._ 147 °C corresponding intensity functions: (a) **M1**, (b) **M2**, (c) **M3**, and (d) **M4**.

The other peaks are at about 5, 8, and 10 Å which are summarized in semi-quantitative plots. The peaks of ~5 Å might be the distances between the molecular origins which arranged the molecules perpendicular or parallel to the neighboring chains. The significant peak shift from 5 to 5.8 Å of **M1** and **M2** determine the intermolecular short-range (see Figure 4.4 zone B) ordering of these two copolymers, in which the peaks attributed to the intra-molecular distances ($r < 3$ Å) (see Figure

4.4 zone A) are superimposed. The intermolecular distance of the third neighbor about 5 Å changes continuously to 5.8 Å, in the cases of **M1** and **M2** (see Figure 4.5 (a) and (b)).

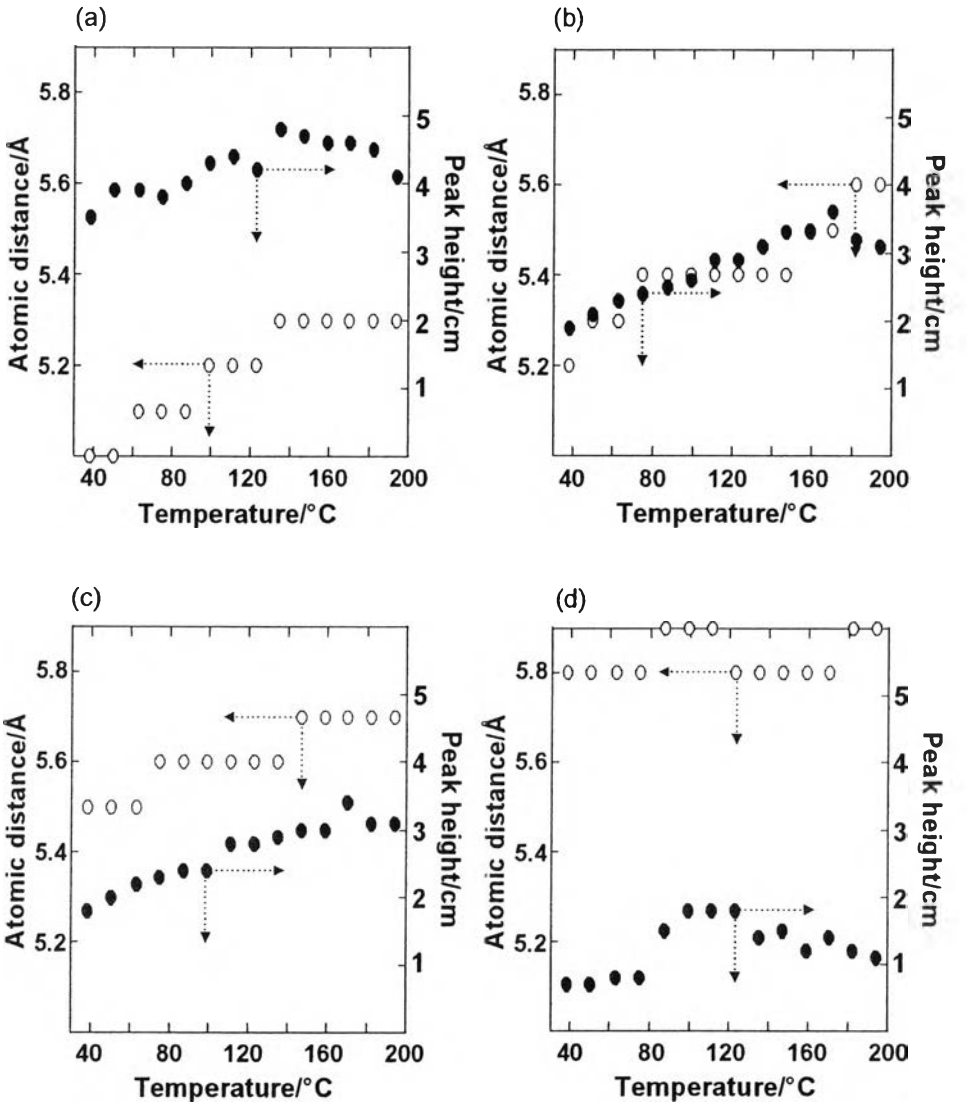

Figure 4.5 Atomic distances (blank) and peak height (solid) of copolymers under various temperatures: (a) **M1**, (b) **M2**, (c) **M3**, and (d) **M4**.

Nevertheless, with the same fluctuated curve patterns, a broad hump in RDF at r > 6 Å (see Figure 4.4 zone C) could not represent the inter-chain ordering of the amorphous copolymers upon heating. No specific inter-atomic distances of r > 6 Å has been explained for these small maxima peaks. The two reasons are as follows:

firstly, the relative position of any part of neighboring repeat units to each other in the amorphous polymer chains is not known, thus only an average disordered configuration can be assumed. Secondly, it is difficult to analyze the relative abundance of any specific inter-atomic spacing to confirm its existence, except assuming all possible random configurations of the polymer chains within the steric limits of the structure. However, the peak for inter-atomic distance ($r > 6$ Å) is further considered with the proton conductivity (see section 3.3).

4.4.3 H-bond based proton transfer in 4-vinylimidazole and acrylic acid copolymer membrane

As resulted in Figure 4.3 (b), the carboxylic acid groups were changed to be unconjugated anhydrides by splitting water molecules out starting from 160 °C for **M3** and from 150 °C for **M4**. It was found that the proton transfer was accelerated along the imidazole-rich copolymer membranes via the weakening in the hydrogen bond network. Above 130 °C, the proton hopping was sufficiently fast as shown by the disappearance of the O-H--N-H stretching peak as seen in Figure 4.6.

The RDF (g(r)) obtained from molecular dynamics simulation and the X-ray scattering calculation of amorphous copolymers shows the peak fluctuation until 5 Å. Based on g(r) calculation, it was reported that the atomic distances belonging to OH--O and NH--N were in the range of 2–3 Å [33–34]. However, in order to clarify the hydrogen bond distance of our copolymers precisely, a molecular dynamics at constant volume (NVT) for 100 ps at various temperatures has to be considered.

Figure 4.6 shows the proton conductivity (σ) of each membrane under the temperature increment. The fact that the conductivity measurement cell has to be set up in the oven and the temperature differences between the inner cell and the oven were quite high, therefore, the measurement above 120 °C was difficult to control. However, it is clear that **M1** and **M2** show an increase in conductivity as the temperature increases and even the temperature reaches 120 °C. In the cases of **M3** and **M4**, the conductivity starts decreasing after 80 °C.

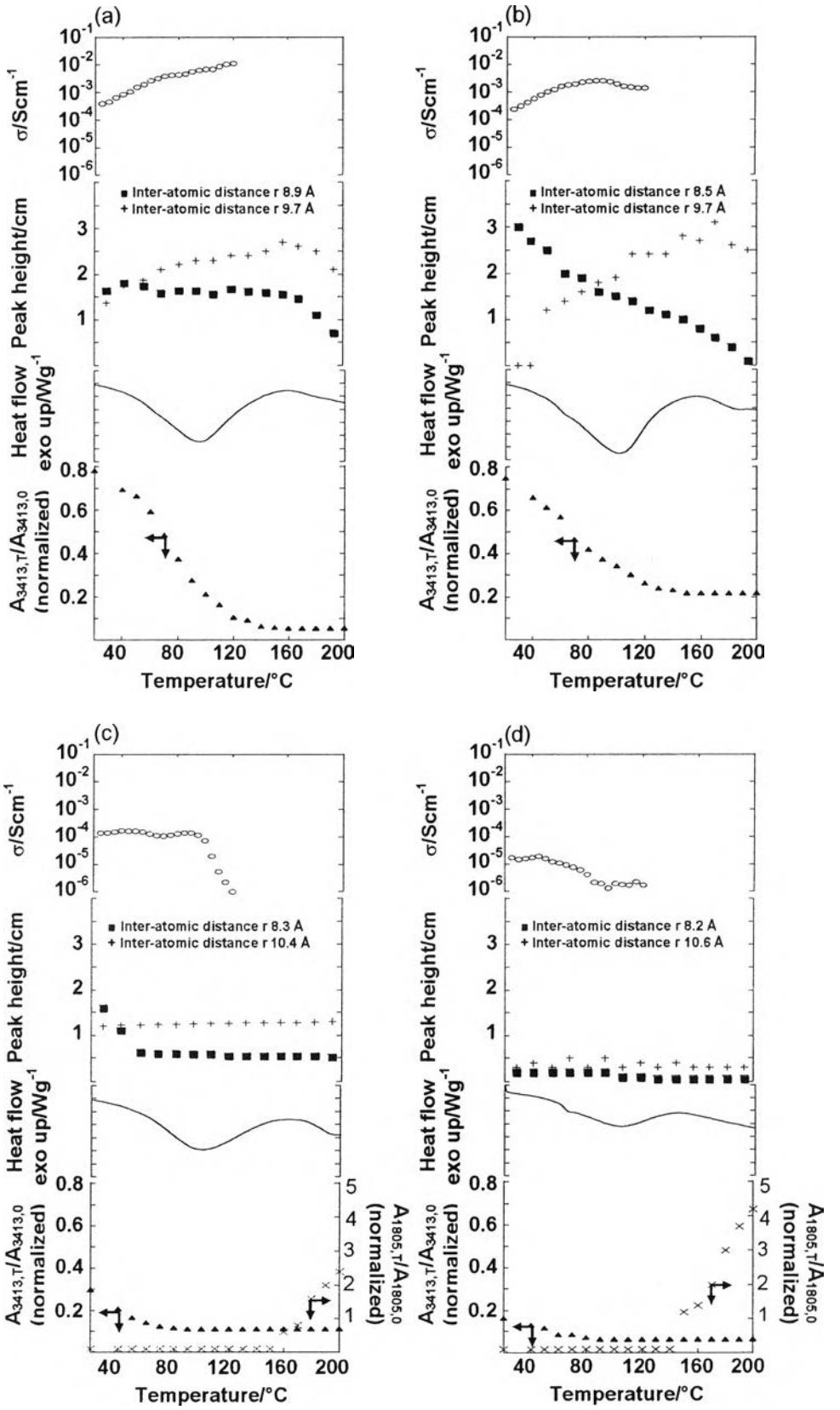

Figure 4.6 Overlay plots of the normalized absorbance at (OH)--N and COO bands, DSC thermograms at first heating cycle, the representative RDF values, and the proton conductivities of copolymers: (a) **M1**, (b) **M2**, (c) **M3**, and (d) **M4**.

Another important point of Figure 4.6 is about the conductivity value. Schuster et al. reported that the imidazole oligomer gave the proton conductivity about 10^{-7}-10^{-4} S/cm [15]. This conductivity could be increased significantly to 10^{-3} S/cm by doping with triflic acid which the functional group is similar to the fluorocarbon chain with sulfonic acid group in Nafion®. Bozkurt et al. showed that a simple mixing system between polyacrylic acid and imidazole aqueous solution gave the membrane with proton conductivity as high as 10^{-3} S/cm [35]. Considering our copolymer system, we suspected that the proton donor-acceptor belonging to carboxylic acid and imidazole groups play an important role of being proton transfer pairing functional group which leads the conductivity to be as high as 10^{-3} S/cm (see Figure 4.6 (a)-(d)). It is also possible that the existence of hydrochloric acid from 1% hydrochloric acid/water (v/v) solution during membrane preparation might consequently enhance the proton conductivity.

The significant changes of inter-atomic distances in the cases of **M1** and **M2** (see Figure 4.6 (a) and (b)) are the peaks at 8.9 and 9.7 Å. These two peaks were plotted with temperature to find that the increase in temperature reduces the peak at 8.9 Å but enhances the peak at 9.7 Å (see Figure 4.6 (a)). When the proton conductivity was overlaid with the RDF values, the changes of both inter-atomic distance and the increase in proton conductivity are relevant to each other. It should be noted that the quantitative peak area of OH--NH at 3413 cm^{-1} is also relevant to the changes of inter-atomic distances. Combining with endothermic peak observed from DSC, we suspect the relationship between the structure and conductivity as follows. The membranes exhibited a very broad endothermic peak between 50 and 150 °C (maximum at 89-103 °C), which might be due to the loss of hydrogen-bond bound water; as a consequence of micro-Brownian motion [36–37]. When the temperature increased, the OH--NH belonging to acrylic acid and imidazole groups started weakening due to the thermal vibrational energy especially from 60 °C. During that time, the polymer rearranged their packing from a favorable inter-atomic distance 8.9 Å to another distance (9.7 Å). The rearrangement of chain packing together with a gradual decrease of OH--HN bond accelerated the proton transfer between the chains before the changes in chain packing could no more favor the OH--NH bond at around 120 °C. There, the analysis of inter-atomic distance allows us to

predict the proton transfer at the very high temperature (above the temperature measured in this work). For example, as one can clearly see that the inter-atomic distance of 9.7 Å decreases significantly after 150 °C (see Figure 4.6 (a) and (b)), it can be mentioned that the conductivity should be decreased above this temperature.

For **M3** and **M4**, as discussed in Figure 2 and 3, only the changes of the unconjugated anhydride peak are observed. In similar, the overlay plots were done (see Figure 4.6 (c) and (d)) to find that both **M3** and **M4** show the endothermic peak while the anhydride formation as identified from the peak at 1805 cm^{-1} becomes stronger. Even though, a trial to plot the peaks at 8.2~8.3 Å and 10.4~10.6 Å were done. It should be noted that the significant changes of the inter-atomic distances for **M3** and **M4** are hardly observed. Here, it should be mentioned that the inter-atomic distance is the information about the packing structure. In the cases of **M1** and **M2**, the inter-atomic distance reflected the hydrogen bond between carboxylic acid and imidazole groups as it involved with the packing structure. However, for **M3** and **M4**, as the copolymer content was not under a favorable condition for hydrogen bond network, the inter-atomic distance reflected the van der Waals based packing structure. As a result, the inter-atomic distances of ~ 8 and ~ 10 Å remain unchanged in the temperature range where the conductivity decreased.

4.5 Conclusion

A systematical study of 4(5)-vinylimidazole and acrylic acid copolymer with different 4(5)-vinylimidazole and acrylic acid contents based on the changes in structure related to the temperature using thermal treatment accessories equipped with FTIR and WAXD including the RDF calculation enabled us to investigate how chain mobility and hydrogen bond initiated the proton conductivity in the membrane. In the case of an ideal alternating copolymer structure of **M1** and **M2**, the hydrogen bond between acrylic acid and imidazole was formed. However, during the heat the intra-molecular distances were changed while the hydrogen bond favored the proton transfer. When the temperature exceeds 120 °C, the hydrogen bond drastically lost.

For the copolymer with more amount of acrylic acid, an unconjugated anhydride was formed during the heat. As a consequence, the proton conductivity was rather low and tended to decrease with an increase in temperature as compared to the alternating copolymer structure one.

4.6 Acknowledgements

The authors gratefully acknowledge the research funding from the Joint Research Program between the National Research Council of Thailand and the Japan Society for the Promotion of Science (NRCT-JSPS). We would like to thank the National Metal and Materials Center-Chiang Mai University (MTEC-CMU) for the scholarship, and the Fuel Cell Research Unit, Chulalongkorn University, for the support.

4.7 References and Notes

[1] P. Commer, A.G. Cherstevy, E. Spohr, A.A. Kornyshev, Fuel Cells 2 (3-4) (2002) 127.

[2] P. Choi, N.H. Jalani, R. Datta, J. Electrochem. Soc. 152 (2005) E123.

[3] M. Tsuda, N.B. Arboleda, H. Kasai, Chem. Phys. 324 (2006) 393-397.

[4] C. Wieser, Fuel Cells 4 (2004) 245.

[5] P. Choi, N.H. Jalani, T.M. Tamphan, R. Datta, J. Polym. Sci., Part B: Polym. Phys. 44(16) (2006) 2183.

[6] H. Xu, Y. Song, H.R. Kunz, J.M. Fenton, J. Power Sources 159 (2006) 979.

[7] Y. Shao, G. Yin, Z. Wang, Y. Gao, J Power Sources 167 (2007) 235.

[8] G. Marsh, Mater. Today (2003) 38-43.

[9] S. Scheiner, M. Yi, J. Phys. Chem. 100 (1996) 9235.

[10] W. Munch, K.D. Kreuer, W. Silvestri, J. Maier, G. Seifert, Solid State Ionics 145 (2001) 437.

[11] C. Yang, P. Costamagna, S. Srinivasan, J. Benziger, and A.B. Bocarsly, J. Power Sources 103 (2001) 1.

[12] A. Bozkurt, and W.H. Meyer, Solid State Ionics 138 (2001) 259.

[13] H. Pu, W.H. Meyer, and G. Wegner, Macromol. Chem. Phys. 202 (2001) 1478.

[14] D. Mercerriyes, H. Grande, O. Miguel, E. Ochoteco, R. Marcilla, and I. Cantero, Chem. Mater. 16 (2004) 604.

[15] M. Schuster, W.H. Meyer, G. Wegner, H.G. Herz, M. Ise, M. Schuster, K.D. Kreuer, and J. Maier, Solid State Ionics 145 (2001) 85.

[16] A. Bozkurt, B. Karadedeli, React. Funct. Polym. 67 (2007) 348.

[17] A. Bozkurt, W.H. Meyer, G. Gutmann, G. Wegner, Solid State Ionics 164 (2003) 169.

[18] K.P. Sao, B.K. Samantaray, S. Bhattacherjee, J Appl. Polym. Sci. 52 (1994) 1917-1923.

[19] M. Jithunsa, K. Tashiro, S.P. Nunes, and S. Chirachanchai, Polym. Degrad. Stab. 93 (2008) 1389-1395.

[20] T. Hashida, K. Tashiro, Polymer 48 (2007) 7614.

[21] D. Lin-Vien, N.B. Colthup, W.G. Fateley, Jeanette, The Handbook of Infrared and Raman Characteristic Frequencies of Organic Molecules, Academic Press, USA, 1991, Ch. 9.

[22] J.T. Daycock, G.P. Jones, J.R.N. Evans, J.M. Thomas, Nature 218 (1968) 673.

[23] A.Kawala, A.R. McGhie, M.M. Labes, J. Chem. Phys. 52 (1970) 3121.

[24] N.S. Murthy, H. Minor, Polymer 31 (1990) 996.

[25] G.R. Mitchell, R. Lovell, A.H. Windle, Polymer 21 (1980) 989.

[26] Y.K. Ovchinikov, Y.M. Antipov, G.S. Markova, Vysokomol. Soyed. A17 (1975) 2081.

[27] C.S. Wang, G.S.Y. Yeh, Polymer 23 (1982) 505.

[28] G.D. Wignall, G.W. Longman, J. Mater. Sci. 8 (1973) 1439.

[29] G.W. Longman, R.P. Sheldon, G.D. Wignall, J. Mater. Sci. 11 (1976) 1339.

[30] L.E. Alexander, X-Ray Diffraction Methods in Polymer Science, John Wiley & Sons, Inc., USA, 1969, Ch. 6.

[31] M. Mondello, H.-J. Yang, H. Furuya, and R.-J. Roe, Macromolecules 27 (1994) 3566.

[32] Y.A. Makhnovskii, Y.K. Ovchinnikov, and A.A. Ovchinnikov, Polymer Science U.S.S.R. 22 (1981) 2801.

[33] U. Trommsdorff, I. Tomka, Macromolecules 28 (1995) 6138.

[34] T. Li, A. Wlaschin, P.B. Balbuena, Ind. Eng. Chem. Res. 40 (2001) 4789.

[35] A. Bozkurt, W.H. Meyer, and G. Wegner, J Power Sources 123 (2003) 126.

[36] M. Eikerling, A.A. Kornyshev, and E. Spohr, Adv. Polym. Sci. 215 (2008) 15.

[37] D. Braun, H. Cherdron, M. Rehahn, H. Ritter, and B. Voit, Polymer Synthesis: Theory and Practice Fundamentals, Methods, Experiments, Springer Berlin Heidelberg New York, Germany, 2005, Ch. 1.